In Situ Vibrational Spectroscopy Studies of Supported Niobium Oxide Catalysts

Loyd J. Burcham,[†] Jerzy Datka,[‡] and Israel E. Wachs*,[†]

Department of Chemical Engineering and Zettlemoyer Center for Surface Studies, Lehigh University, Bethlehem, Pennsylvania 18015, and Faculty of Chemistry, Jagiellonian University, ul. R. Ingardena 3, 30-060 Krakow, Poland

The IR spectra of bulk $Nb_2O_5 \cdot nH_2O$ and niobia supported on SiO_2, Al_2O_3, ZrO_2, and TiO_2 were recorded in the fundamental and overtone Nb═O regions, as well as in the hydroxyl region, to develop a better understanding of the structural models of surface NbO_x species. The coincidence of the IR and Raman fundamental Nb═O frequency in Nb_2O_5/Al_2O_3, Nb_2O_5/ZrO_2, and Nb_2O_5/TiO_2 provides the strongest evidence that the NbO_x surface species (Nb═O fundamental at 980 cm^{-1}) is present as a mono-oxo moiety. The IR and Raman band positions would not be coincident for a di-oxo species. This conclusion is further supported by the presence of only a single overtone at ~1960 cm^{-1} (2 × 980 cm^{-1}) in Nb_2O_5/ZrO_2 and Nb_2O_5/TiO_2 and the presence of the most intense overtone at 1966 cm^{-1} in Nb_2O_5/Al_2O_3. Lower frequency IR fundamentals at 880 cm^{-1} (low loading) and 935 cm^{-1} (high loading) are also seen in Nb_2O_5/ZrO_2, and the IR overtone region of Nb_2O_5/Al_2O_3 exhibited weak bands at ~1870 cm^{-1} (935 cm^{-1} overtone) and 1914 cm^{-1} (935 + 980 cm^{-1} combination). These fundamental niobia bands at 880 and 935 cm^{-1}, which are also observed in Raman for NbO_x surface species on alumina, zirconia, and titania, are assigned to an Nb─O─Nb stretching mode, $\nu_s([-O-Nb-O-]_n)$, that shifts from 880 to 935 cm^{-1} with increased loading. Finally, observation of the hydroxyl region indicates that the higher frequency surface hydroxyls on the SiO_2, Al_2O_3, ZrO_2, and TiO_2 supports are generally titrated preferentially as niobia loading is increased. Also, in Nb_2O_5/ZrO_2 and Nb_2O_5/TiO_2 a new (nonacidic or weakly acidic) Nb─OH or Nb─OH─Zr (Nb─OH─Ti) surface hydroxyl group is created at 3710−3730 cm^{-1} that is very similar in frequency to the Nb─OH band observed in bulk $Nb_2O_5 \cdot nH_2O$ at 3702 cm^{-1}.

Introduction

Niobia-containing catalysts have received attention in recent years due to their catalytic activity in selective oxidation, acid-catalyzed hydrocarbon conversions, hydrotreating, hydrogenation/dehydrogenation, photo- and electrocatalysis, and polymerization.[1−5] In particular, supported niobia catalysts, which consist of an active two-dimensional niobia overlayer that is 100% dispersed on a high surface area support (Al_2O_3, TiO_2, ZrO_2, and SiO_2), were shown to have significant Lewis and Brønsted acidity.[5−10] The acidity of these supported niobia surface species is believed to be responsible for the significant activity and selectivity enhancement observed in selective catalytic reduction (SCR) of NO_x with NH_3 over (Nb_2O_5 + V_2O_5)/TiO_2 catalysts, relative to V_2O_5/TiO_2 catalysts.[11] However, at elevated temperatures Nb_2O_5/TiO_2 is active for the SCR reaction in the absence of vanadia—indicating that the niobia surface species on titania have some redox properties in addition to their acid properties.[5,11] Also, Nb_2O_5/SiO_2 catalysts exhibit redox behavior for the selective oxidation of methanol to formaldehyde, in which 90% selectivity to formaldehyde is achieved.[11−13] It has been suggested that the bridging Nb─O─support bond is the bond responsible for both the acid[6−8,14] and redox[11,13] properties of supported niobia catalysts, but detailed fundamental information about the molecular structures of the supported niobia surface species still remains incomplete in the literature.

Molecular structural characterization studies of supported niobia catalysts have mainly included Raman spectroscopy[15−20] and X-ray absorption near-edge spectroscopy (XANES)/extended X-ray absorption fine structure (EXAFS).[10,20−28] Raman and EXAFS provide information on the number and types of niobium─oxygen bonds present in the niobia surface species (Nb═O, O═Nb═O, Nb─O─Nb, Nb─O─support, etc.), whereas XANES provides coordination information (NbO_4, NbO_6, etc.). According to the papers by Jehng and Wachs[15] and Pittman and Bell,[17] the dehydrated Raman spectra of niobia supported on Al_2O_3, TiO_2, ZrO_2, and SiO_2 exhibit bands in the region ~825 to ~980 cm^{-1} that are assigned to the vibrational modes of NbO_x surface species. Silica-supported Nb_2O_5, which is limited to loadings below $^1/_2$ monolayer due to the low surface reactivity of the silica support, possesses only a single Raman band at ~980 cm^{-1}, which is assigned to a mono-oxo, Nb═O stretching vibration. This same Nb═O stretching band also appears at ~980 cm^{-1} in the Raman spectra of niobia supported on Al_2O_3, ZrO_2, and TiO_2 for both low and high loadings, except that at the lower loading of Nb_2O_5/ZrO_2 this vibrational mode occurs at ~956 cm^{-1}. Additional niobia bands in the Raman spectra of these catalysts include a peak at ~825−883 cm^{-1} for low loadings of niobia on alumina and zirconia, as well as a band at ~935 cm^{-1} for high loadings of niobia on alumina, zirconia, and titania. These lower frequency stretching bands have been assigned to Nb═O bonds within different isolated or polymerized NbO_x surface species.[15,17] For the high loadings of Nb_2O_5/Al_2O_3, another new band appears at ~647 cm^{-1} that is characteristic of the stretching mode of Nb─O─Nb polym-

* Corresponding author.
† Lehigh University.
‡ Jagiellonian Univeristy.

erized bonds[17] (the Raman region from ~600 to 700 cm^{-1} is obscured by the strong vibrations of the TiO_2 and ZrO_2 supports[15]). Therefore, Raman spectroscopy indicates the existence of both Nb=O and Nb—O—Nb bonds within the molecular structure of supported NbO_x surface species, the ratio of polymeric to monomeric species increasing with niobia loading.

The EXAFS studies similarly indicate the presence of Nb=O and Nb—O—Nb structural moieties, as well as Nb—O—support bonds, in supported niobia surface species. However, there is disagreement between the Raman and EXAFS conclusions regarding the number of doubly bonded oxygen atoms attached to the niobium atoms. Specifically, the EXAFS data (Nb K-edge) for 5 wt % Nb_2O_5/Al_2O_3 were best fit by Tanaka et al.[23] using di-oxo O=Nb=O moieties, instead of the mono-oxo Nb=O units suggested by Raman studies. Several papers by Iwasawa and co-workers also place a di-oxo O=Nb=O unit on niobia surface monomers in Nb_2O_5/SiO_2 catalysts[10,20,22] and Nb_2O_5/Al_2O_3 catalysts[20] based on EXAFS curve-fitting analyses. However, for niobia dimers on silica (prepared with a different precursor than the monomers)[10,22,26] and for niobia monomers on titania[20] these same authors report mono-oxo Nb=O units. Yoshida et al.[24,25] found only mono-oxo Nb=O moieties as monomers and oligomers in the EXAFS of Nb_2O_5/SiO_2 prepared by the equilibrium adsorption method. Finally, Kobayashi et al.[28] conclude from quantum chemical calculations and EXAFS data that a mono-oxo niobia species is most stable on silica but that a di-oxo species is more stable on alumina. The discrepancies in mono-oxo versus di-oxo structures found within the EXAFS studies of Nb_2O_5/SiO_2 catalysts are especially puzzling in light of the fact that Wachs et al.[11,13] found the molecular structures of surface niobia species to be independent of preparation method (oxalate, alkoxide, or allyl).

Less ambiguous is the coordination of the NbO_x surface species, which has been obtained from XANES experiments.[20-25] The relatively high XANES preedge peak intensity (Nb K-edge) indicates a 4-fold coordination for niobia on silica[21-22,24-25] and for low loadings of niobia on alumina.[20-21,23] Higher loadings of niobia on alumina exhibit a preedge intensity that is significantly lower and is characteristic of the six-coordinated niobium in a niobic acid-like species.[21,23]

Several other characterization techniques have also been applied to supported niobia catalysts. For instance, Ko et al.[29-31] used X-ray diffraction (XRD) and high-resolution transmission electron microscopy (HRTEM) to demonstrate that monolayer dispersions of niobia are achievable on silica, while Tanaka et al.[32] used UV—vis diffuse reflectance spectroscopy to distinguish between niobia monomers and oligomers on silica. Also, X-ray photoelectron spectroscopy (XPS) has indicated that the niobia surface species present on high surface area oxide supports are in the fully oxidized, Nb^{5+} valence state.[16,20] To a lesser extent, both infrared (IR) and electron spin resonance (ESR) spectroscopies have been employed to probe the nature of organic Nb precursors used in certain preparation methods.[20,33] Curiously, the only IR spectra found in the literature for supported niobia catalysts after calcination appear in the work of Burke and Ko[8] as ambient, hydrated diffuse reflectance (DRIFT) spectra of Nb_2O_5/SiO_2. Such a lack of infrared data has been unfortunate because differences in the IR and Raman selection rules can be used to resolve molecular structural issues if the complementary IR and Raman spectra are both available.[34] In the present study, therefore, infrared spectroscopy is employed to further elucidate the molecular structures of supported niobium oxide catalysts under in situ, dehydrated conditions (molecular structures under ambient, hydrated conditions can

TABLE 1: Nb_2O_5 Loadings on Various Supports

support	low loading	high loading
SiO_2	1 wt % (6% of monolayer)^a	2 wt % (12% of monolayer)^a
Al_2O_3	5 wt % (26% of monolayer)	15 wt % (80% of monolayer)
ZrO_2	1 wt % (20% of monolayer)	5 wt % (100% of monolayer)
TiO_2	3 wt % (43% of monolayer)	7 wt % (100% of monolayer)

^{a} By analogy to the vanadia/silica monolayer (2.6 V atoms/nm^2),[38] monolayer coverage (2.6 Nb atoms/nm^2) is expected to be roughly 16 wt % Nb_2O_5/SiO_2.

be found elsewhere[16]). In particular, the issue of mono-oxo versus di-oxo terminal oxygen species will be addressed in an effort to resolve the contradicting conclusions obtained from EXAFS and Raman data concerning this topic.

Finally, the interaction of niobia with support hydroxyls is also considered in the present investigation. Previous authors[7,17,33,35-38] found that deposition of acidic oxides on basic oxide supports generally proceeds via an acid—base titration of the support surface hydroxyls with the oxo-anions of the deposited oxide, resulting in a decrease in the IR intensity of the support hydroxyls. In the case of alumina, the high-frequency OH bands associated with more basic hydroxyls were preferentially consumed as the loading of niobia was increased.[7,35] Deposition of chromia on alumina, titania, zirconia, and silica,[35] and of vanadia on silica,[38] showed the same preferential titration of high-frequency, basic hydroxyls. Conversely, the Raman spectra of the hydroxyl region of Nb_2O_5/TiO_2 appear to show preferential titration of the two lower frequency hydroxyls.[17] In all cases it was impossible to achieve complete titration of the support hydroxyls, even at monolayer loadings, indicating the inaccessibility or nonreactivity of the remaining OH groups.[7,17,35-38] The present study will reexamine this issue over a greater range of supported niobia catalysts.

The IR spectra of the following materials are examined in this study: bulk hydrated niobia ($Nb_2O_5 \cdot nH_2O$, also called niobic acid), pure oxide supports, and niobia supported at both low loadings (20—43% of monolayer) and high loadings (80—100% of monolayer). A list of these oxides and the loadings of niobia investigated is given in Table 1, where the monolayer coverage of Nb_2O_5/SiO_2 is projected to be roughly 16 wt % niobia (2.6 Nb atoms/nm^2) based on analogy with recently achieved monolayer dispersions of vanadia on silica.[38] Monolayer niobium surface densities[37] on the more reactive surfaces of alumina, titania, and zirconia are approximately 5 Nb atoms/nm^2.

Experimental Section

The supported niobia samples were prepared by aqueous impregnation methods using niobium oxalate (Niobium Products Co., Pittsburgh, PA) as a precursor.[15] Oxide supports consisted of Al_2O_3 (180 m^2/g; Harshaw), TiO_2 (50 m^2/g; Degussa P-25), ZrO_2 (39 m^2/g; Degussa), and SiO_2 (275 m^2/g; Cab-O-Sil). After impregnation with the niobium oxalate/oxalic acid aqueous precursor, the samples were dried at room temperature for 16 h, then dried at 120 °C for another 16 h, and finally calcined at 450 °C (Nb_2O_5/TiO_2 and Nb_2O_5/ZrO_2; 2 h) or at 500 °C (Nb_2O_5/Al_2O_3 and Nb_2O_5/SiO_2; 16 h) under flowing dry air. Bulk hydrated niobium oxide, $Nb_2O_5 \cdot nH_2O$ (100 m^2/g), was provided by Niobium Products Co. and is stable to about 350 °C. Infrared spectra were obtained by pressing the powdered catalyst into self-supporting wafers (~5—45 mg) and mounting the samples in an in-situ FTIR cell (Harrick HTC-100). Spectra were recorded with a BioRad FTS-40A FTIR spectrometer (DTGS detector) using 250 signal-averaged scans at a resolution of 2

IR Spectra of Niobium Oxide Catalysts

J. Phys. Chem. B, Vol. 103, No. 29, 1999 **6017**

TABLE 2: IR and Raman Band Frequencies (cm^{-1}) for Bulk and Supported Niobia in the Fundamental and Overtone Niobium–Oxygen Stretching Regions (Raman Data Taken from refs 39 and 15 for Bulk and Supported Niobia, Respectively)^a

	assignment	Nb$_2$O$_5$·nH$_2$O	Nb$_2$O$_5$/SiO$_2$	Nb$_2$O$_5$/Al$_2$O$_3$	Nb$_2$O$_5$/ZrO$_2$	Nb$_2$O$_5$/TiO$_2$
Raman	$\nu_1 = \nu_s$(Nb=O)	980	988–988	980–988	956–988	983–985
	$\nu_2 = \nu_s$([–O–Nb–O–]$_n$)	930	–	883–935	823–935	935
IR fund	ν_1	b	b	~980	965–986	980–980
	ν_2	b	b	b	880–925	955–955
IR over.	$2\nu_1$	1986	b	1947–1966	1929–1953	1959–1959^c
	$2\nu_2$, ($\nu_1 + \nu_2$)	b	b	1870, 1914	b	b

^{a} First number corresponds to low loading; second number corresponds to high loading. ^{b} Cannot be determined due to strong absorbance by the support and/or weak niobia absorbance. ^{c} An additional overtone band at 1986 cm^{-1} in Nb$_2$O$_5$/TiO$_2$ is assigned to bulk Nb$_2$O$_5$·nH$_2$O (see text).
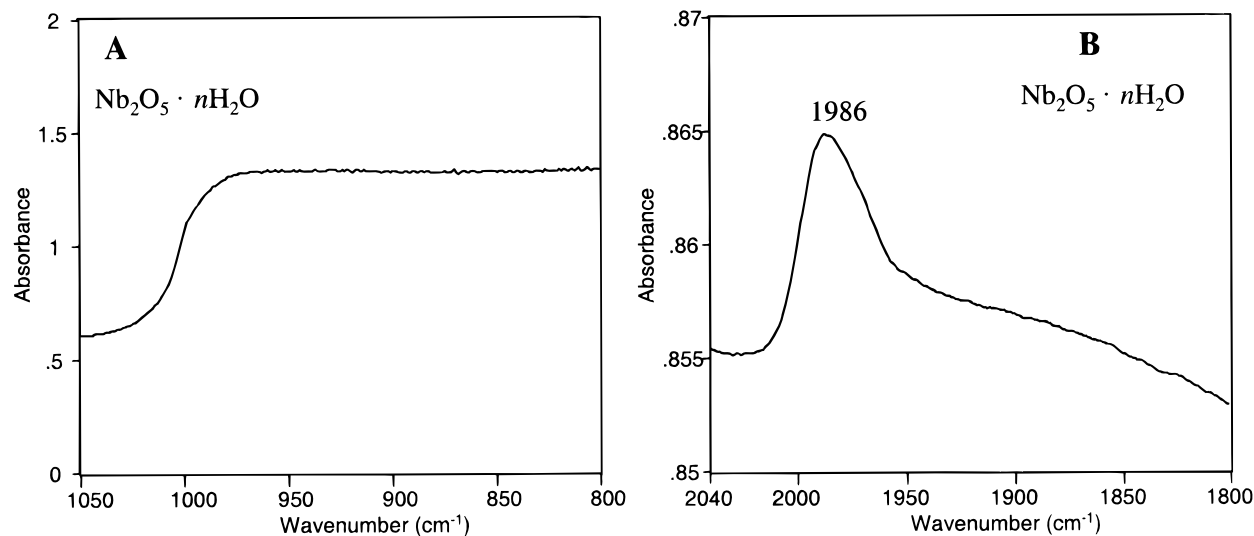
Figure 1. Fundamental (A) and overtone (B) IR spectra of Nb$_2$O$_5$·nH$_2$O. The ordinate scale has been expanded in the overtone spectrum for clarity.

cm^{-1}. All spectra were normalized to 10 mg and smoothed (Savitsky-Golay algorithm; degree 2 with 20 pts) to enhance the apparent signal-to-noise ratio. The pretreatment inside the IR cell consisted of first heating the sample to 350 °C in a vacuum (~10^{-4} to 10^{-5} Torr) followed by cooling to 50 °C for spectrum acquisition.

Results

1. Fundamental Nb=O Bands. The fundamental region of the IR spectra of bulk Nb$_2$O$_5$·nH$_2$O, Nb$_2$O$_5$/Al$_2$O$_3$, Nb$_2$O$_5$/ZrO$_2$, and Nb$_2$O$_5$/TiO$_2$ are presented in Figures 1A–4A, and band positions are summarized in Table 2. The analysis of the spectra in this region is difficult because of high absorption of the IR radiation by the oxide supports below ~1000 cm^{-1} (SiO$_2$), ~950 cm^{-1} (Al$_2$O$_3$ and TiO$_2$), and ~800 cm^{-1} (ZrO$_2$). In the case of SiO$_2$, the observation of the Nb=O fundamental was not possible. For bulk Nb$_2$O$_5$·nH$_2$O, the Nb=O fundamental band that appears in the Raman spectrum[39,40] at ~980 cm^{-1} is also not seen in IR (see Figure 1A)—only a "step" at about ~970 cm^{-1} is present.

In Nb$_2$O$_5$/Al$_2$O$_3$ (Figure 2A), the spectra do not show any distinct bands in the fundamental region, but a band about ~980 cm^{-1} that can be assigned to the Nb=O fundamental is present in the difference spectra (spectra of Nb$_2$O$_5$/Al$_2$O$_3$ minus the spectrum of Al$_2$O$_3$; Figure 2A-d,e). A similar band (~980–988 cm^{-1}) was observed in the Raman spectra.[15,18] The Nb=O fundamental band is well seen in the spectra of Nb$_2$O$_5$/ZrO$_2$ (Figure 3A). The increase in niobia loading resulted in a shift of the band from 965 to 986 cm^{-1} and broadening of the band. Similar shifts from 956 to 988 cm^{-1} were observed in the Raman spectra.[15] Another band at 880 cm^{-1} is present in Nb$_2$O$_5$/ZrO$_2$

at low loading, but this band disappears at higher loadings. Similar phenomena were also observed in the Raman spectra. The Raman spectrum of higher loading Nb$_2$O$_5$/ZrO$_2$ also showed a distinct band at ~935 cm^{-1}. This band is very poorly seen in the present IR spectra but can be better observed as a weak band at ~925 cm^{-1} after baseline correction (see Figure 3C). The spectra of Nb$_2$O$_5$/TiO$_2$ (Figure 4A) show a broad, but defined, band at ~980 cm^{-1} for the Nb=O fundamental that is coincident with a similar band in Raman (983–985 cm^{-1}).[15,17] Baseline subtraction also shows a shoulder at ~955 cm^{-1} (Figure 4C), but the exact position of this shoulder may be distorted due to the weakness and broadness of the original band before baseline correction. Within these experimental limitations, this band is probably coincident with the broad Raman band[15,17] found at 940 cm^{-1}.

2. Overtone Nb=O Bands. The infrared spectra in the Nb=O overtone region of bulk Nb$_2$O$_5$·nH$_2$O, Nb$_2$O$_5$/Al$_2$O$_3$, Nb$_2$O$_5$/ZrO$_2$, and Nb$_2$O$_5$/TiO$_2$ are presented in Figures 1B–4B, and overtone band positions are summarized in Table 2. These niobia overtones are generally more distinctive than the corresponding fundamentals because the supports do not absorb significantly in this infrared region, in contrast to the strong support absorption in the fundamental region. However, the overtones are also much weaker than the fundamentals (compare ordinate scales in Figures 1–4). The Nb=O overtones could not be seen in Nb$_2$O$_5$/SiO$_2$ due to the presence of strong bands from silica (1870 and 1990 cm^{-1}) in this region. The Nb=O overtone of bulk Nb$_2$O$_5$·nH$_2$O is observed at 1986 cm^{-1} and is a much more distinctive band than the fundamental. In Nb$_2$O$_5$/Al$_2$O$_3$, an overtone band is present at 1947 cm^{-1} that shifts to 1966 cm^{-1} with increasing loading (similar to the shift in the fundamental
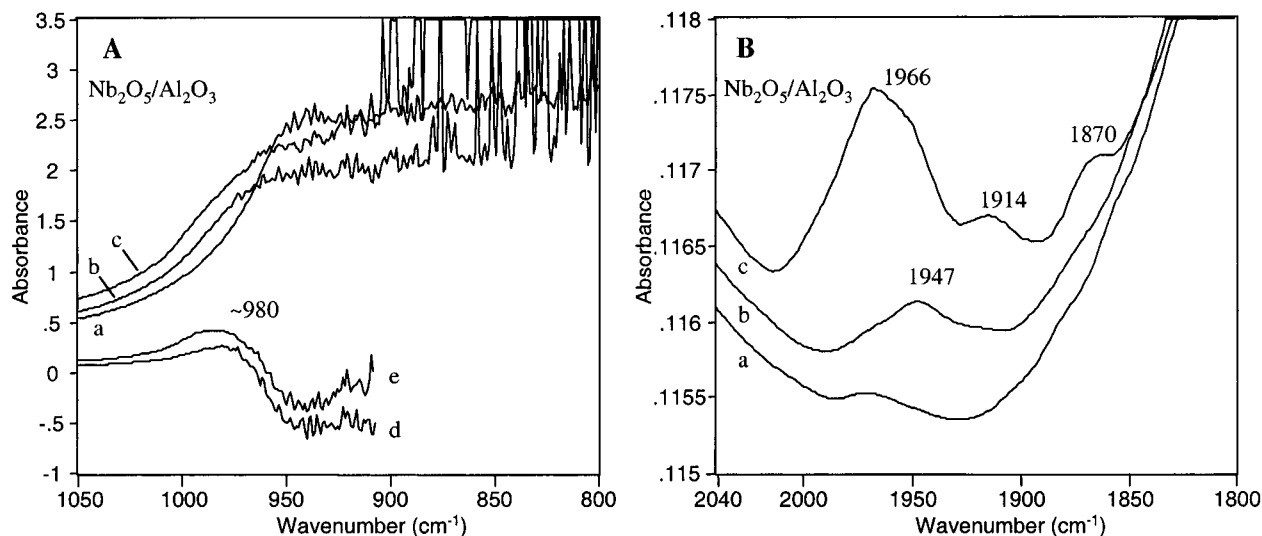
Figure 2. Fundamental (A) and overtone (B) IR spectra of Nb_2O_5/Al_2O_3. The ordinate scale has been expanded in the overtone spectra for clarity. Spectra are labeled as follows: a = Al_2O_3 support; b = 5 wt % Nb_2O_5/Al_2O_3; c = 15 wt % Nb_2O_5/Al_2O_3; d = difference spectrum, (b) − (a); e = difference spectrum, (c) − (a).
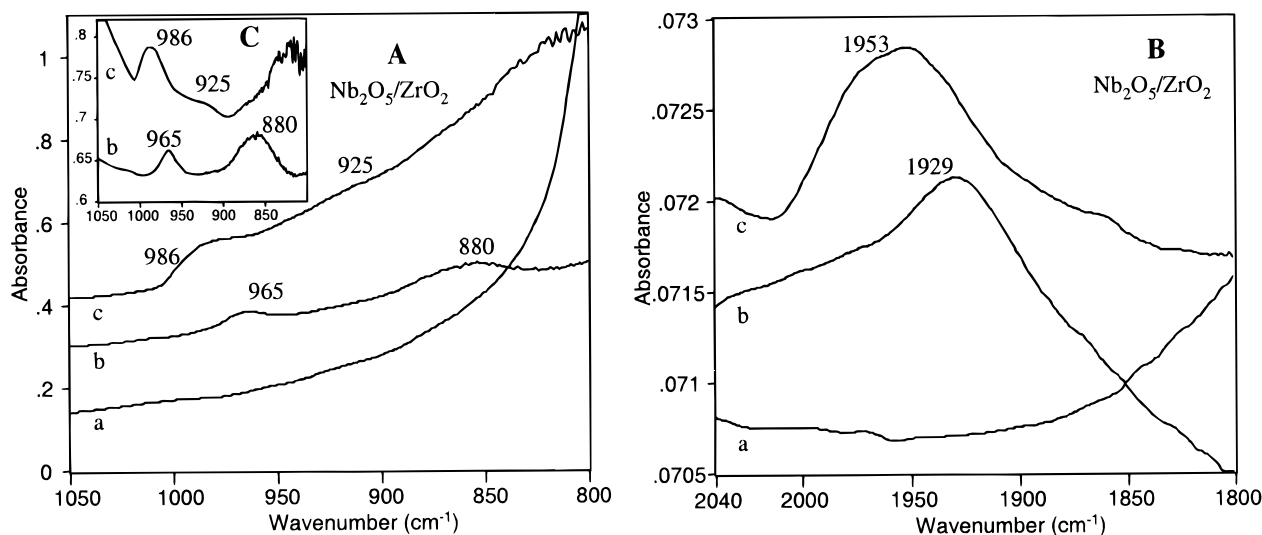
Figure 3. Fundamental (A) and overtone (B) IR spectra of Nb_2O_5/ZrO_2. The ordinate scale has been expanded in the overtone spectra for clarity. The inset (C) shows the baseline-subtracted spectra in the fundamental region. Spectra are labeled as follows: a = ZrO_2 support; b = 1 wt % Nb_2O_5/ZrO_2; c = 5 wt % Nb_2O_5/ZrO_2.

band of the Raman spectra). At higher loadings of Nb_2O_5/Al_2O_3, additional bands are seen at 1870 and 1914 cm^{-1}. A distinct Nb=O overtone band is also seen in Nb_2O_5/ZrO_2. This band shifts to a higher frequency (from 1929 to 1953 cm^{-1}) and broadens with increasing loading. Analogous phenomena were observed in the IR fundamental region (Figure 3A) and in the corresponding Raman spectra.[15]

The spectrum of Nb_2O_5/TiO_2 shows a distinct Nb=O overtone band of supported niobia at 1959 cm^{-1}, as well as a band at 1986 cm^{-1} that is assigned to the overtone band of bulk Nb_2O_5·nH_2O. The Nb_2O_5/TiO_2 overtone at 1959 cm^{-1} did not shift position with loading, and this independence of band position with loading was also observed for the fundamental vibrations in both Raman and IR. Finally, with the exception of Nb_2O_5/TiO_2 and possibly the highest loading of 5 wt % Nb_2O_5/ZrO_2 (overtone shoulder at 1986 cm^{-1}), the presence of bulk Nb_2O_5·nH_2O can be ruled out on the other catalysts based on the absence of an overtone band at 1986 cm^{-1}. The relatively high frequency of this niobic acid IR overtone is clearly distinguishable from the overtones of supported NbO_x surface species,

unlike the 930 and 980 cm^{-1} fundamental Raman bands of niobic acid.

3. Hydroxyl Bands. The interaction of niobia with the oxide support hydroxyl groups can be seen in Figure 5A−D. For the silica support there are isolated Si−OH and geminal Si(OH)$_2$ hydroxyls present on the surface that exhibit IR stretching bands at 3746 and 3743 cm^{-1}, respectively.[35,41] Both bands normally overlap, so only one distinct band is seen in the dehydrated silica spectrum in Figure 5A at 3746 cm^{-1}. The weak shoulder at 3730 cm^{-1} is due to hydrogen-bonded silanols. The deposition of small amounts of niobia (1 wt % Nb_2O_5/SiO_2) did not significantly alter the spectrum, but larger amounts (2 wt % Nb_2O_5/SiO_2) diminished the OH band of the isolated hydroxyls at 3746 cm^{-1} (this band is still seen as a shoulder). The dominant band becomes that of the geminal hydroxyls at 3743 cm^{-1} and indicates that the isolated hydroxyls are more reactive toward niobia. Again, the increase in absorption in the region 3700− 3740 cm^{-1} is most likely due to hydrogen-bonding interactions between silanols and neighboring niobia oxygen atoms, but the appearance of new hydroxyl species cannot be ruled out.

IR Spectra of Niobium Oxide Catalysts

J. Phys. Chem. B, Vol. 103, No. 29, 1999 **6019**
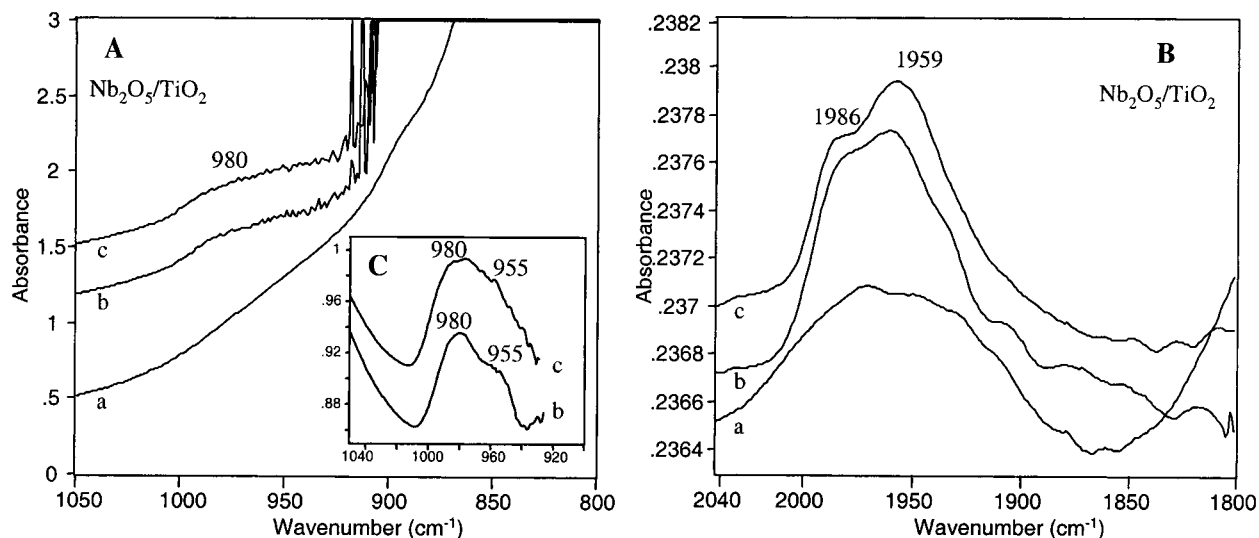
Figure 4. Fundamental (A) and overtone (B) IR spectra of Nb_2O_5/TiO_2. The ordinate scale has been expanded in the overtone spectra for clarity. The inset (C) shows the baseline-subtracted spectra in the fundamental region. Spectra are labeled as follows: a = TiO_2 support; b = 3 wt % Nb_2O_5/TiO_2; c = 7 wt % Nb_2O_5/TiO_2.
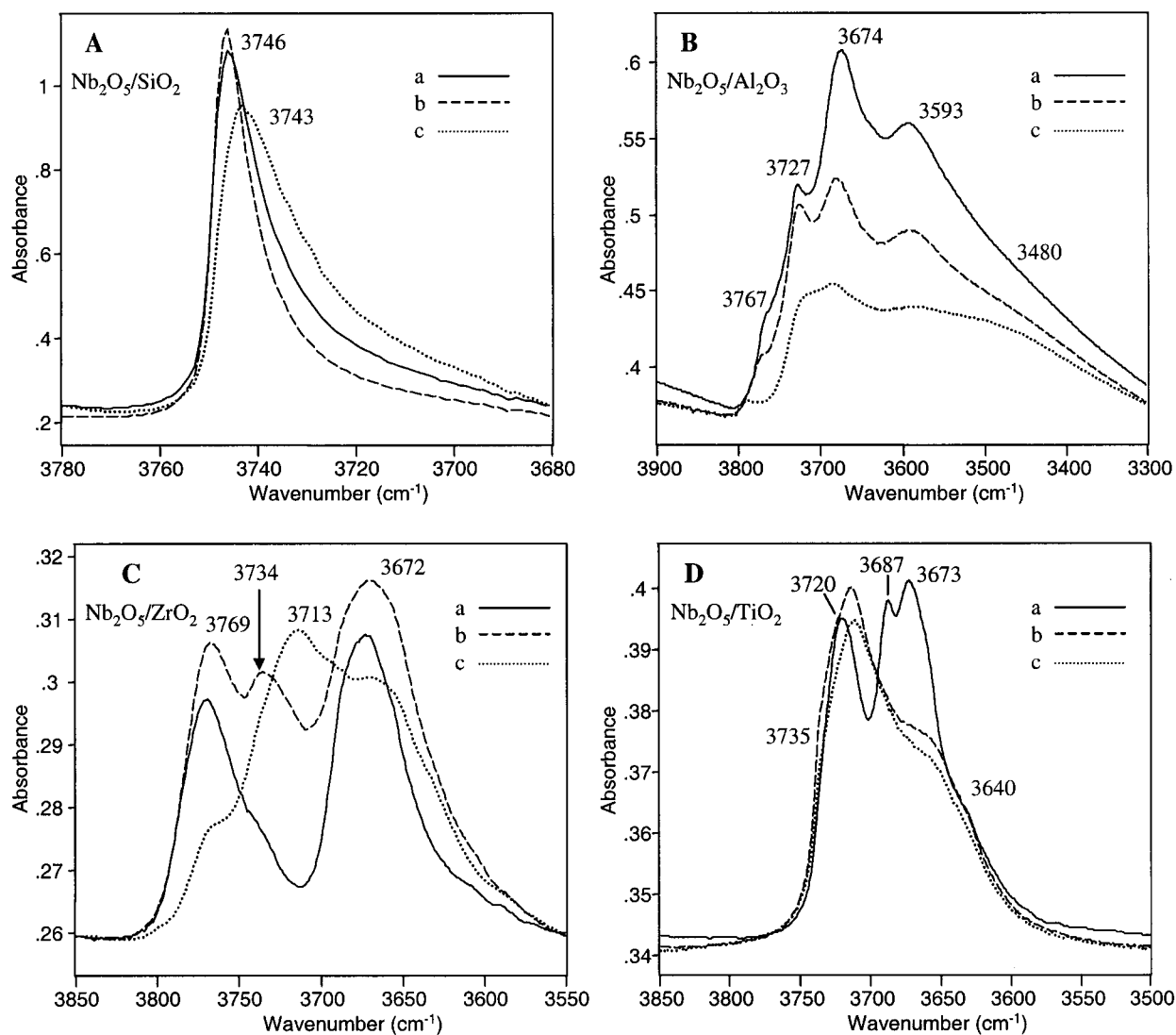
Figure 5. IR spectra of the hydroxyl region of supported niobia catalysts: (A) SiO_2 (a), 1 wt % Nb_2O_5/SiO_2 (b), 2 wt % Nb_2O_5/SiO_2 (c); (B) Al_2O_3 (a), 5 wt % Nb_2O_5/Al_2O_3 (b), 15 wt % Nb_2O_5/Al_2O_3 (c); (C) ZrO_2 (a), 1 wt % Nb_2O_5/ZrO_2 (b), 5 wt % Nb_2O_5/ZrO_2 (c); (D) TiO_2 (a), 3 wt % Nb_2O_5/TiO_2 (b), 7 wt % Nb_2O_5/TiO_2 (c).

The spectrum of dehydrated alumina shows five OH bands at 3480, 3593, 3674, 3727, and 3767 cm^{-1} that have been assigned by Knözinger et al.[42] Generally, the more basic and isolated surface hydroxyls vibrate at higher wavenumbers.[7,35,42]
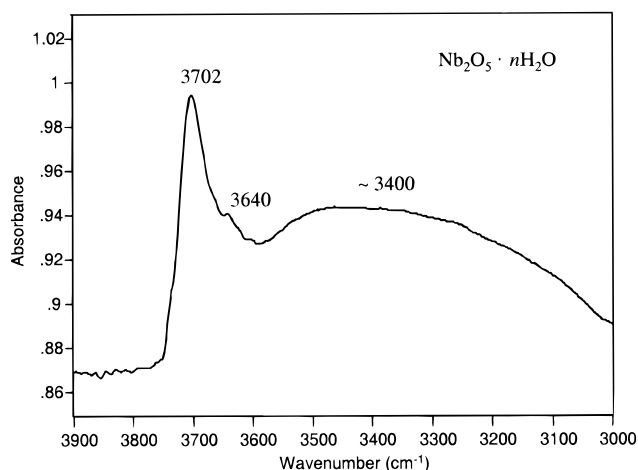
Figure 6. IR spectrum of the hydroxyl region of $Nb_2O_5 \cdot nH_2O$.

Figure 5B shows that the deposition of niobia on alumina diminishes all Al—OH bands. However, at 80% of monolayer coverage (15 wt % Nb_2O_5/Al_2O_3), the high-frequency Al—OH band at 3767 cm^{-1} completely disappears, while the other bands remain at significantly diminished intensities. Such behavior indicates that the most basic hydroxyls are the most reactive upon deposition of niobia.

The hydroxyl region of zirconia displays two bands (see Figure 5C) at 3672 and 3769 cm^{-1}, which have been assigned by Tsyganenko and Filimonov[43] to surface hydroxyls bonded to three and to one Zr atoms, respectively. The deposition of niobia diminished both bands, but the larger decrease in intensity of the band at 3769 cm^{-1} indicates that the hydroxyls bound to a single Zr atom are more reactive with deposited niobia. Of special interest is the appearance of a new band, appearing at 3734 cm^{-1} at low loading but shifting to 3713 cm^{-1} at full monolayer coverage, for which the assignment is unknown. It is possible that this band may be due to Nb—OH isolated hydroxyls or Nb—OH—Zr bridging hydroxyls, especially considering that bulk $Nb_2O_5 \cdot nH_2O$ exhibits a very distinct hydroxyl stretching band at 3702 cm^{-1}, as shown in Figure 6.

Finally, Figure 5D shows the hydroxyl region of the titania-supported niobia catalysts. Pure titania exhibits bands at 3673, 3687, and 3720 cm^{-1}, with shoulders at 3640 and 3735 cm^{-1}, but the assignments of these bands are not clear. Some authors[43,44] assign the 3720 cm^{-1} band to Ti—OH species (bonded to a single Ti atom), while others[35,45] propose that this band originates, at least in part, from Si—OH hydroxyls on silica impurities. Busca et al.[45] have performed the most systematic study of OH vibrations in silica—titania mixed oxides and show that pure titania (anatase) exhibits a band at 3710 cm^{-1} with a shoulder at 3730 cm^{-1}. Upon addition of very small amounts of silica (0.5 mol %) to the titania, the 3710 cm^{-1} band completely disappears and the shoulder at 3730 cm^{-1} shifts to 3735 cm^{-1} and becomes sharper and more pronounced. Additional silica (10 mol %, 25 mol %, etc.) results in domination of the silica hydroxyl band, which systematically shifts to higher frequency (3746 cm^{-1} in pure SiO_2). The authors conclude from this behavior that the 3710 cm^{-1} band represents isolated, "free" Ti—OH groups located on low-coordination surface titanium defect sites. Addition of very small amounts of silica results in substitution of these Ti defect sites by silicon atoms, which, in turn, eliminates the 3710 cm^{-1} Ti—OH band. Likewise, for very low silica content the Si—OH vibrations occur at lower frequencies than in pure silica due to the different silicon environment relative to pure SiO_2.

Therefore, in pure titania (Figure 5D-a) the band at 3720 cm^{-1} is assigned to isolated Ti—OH groups and the shoulder at 3735 cm^{-1} is assigned to trace amounts of silica impurity. Such assignments are also consistent with XPS data on anatase (Degussa P-25) catalysts,[46] which show a very low impurity level of only 0.75 at. % Si on the surface of 1 wt % V_2O_5/TiO_2 (XPS data on pure TiO_2 was not reported). There is also disagreement[35] on the precise assignment of the other hydroxyl bands at 3687, 3673, and 3640 cm^{-1}, but by analogy to hydroxyl vibrations on other oxides it seems likely that these lower-frequency bands represent bridged or hydrogen-bonded Ti—OH species.[43,44] Niobia deposition results in the disappearance of the Ti—OH bands at 3673 and 3687 cm^{-1}, while the band at 3720 cm^{-1} is shifted to 3710 cm^{-1} and broadened. Pittman and Bell[17] observed very similar trends for this catalytic system in the Raman spectra of the hydroxyl region. The shift in the 3720 cm^{-1} band may indicate that a new band has developed at 3710 cm^{-1} in a manner similar to what was observed with Nb_2O_5/ZrO_2. Last, the band at 3640 cm^{-1} persists even at monolayer coverage, indicating that this hydroxyl group is relatively unreactive with deposited niobia.

Discussion

1. Molecular Structures of Supported Niobia Surface Species. A primary objective of the present study is to determine the presence of mono-oxo, Nb=O species versus di-oxo, O=Nb=O species in the niobia surface species present on oxide supports at and below monolayer coverage. This issue may be addressed by observing the number of fundamental (IR and Raman) and overtone (IR) bands in the Nb=O stretching regions (assuming that the Nb=O bonds contain the majority of vibrational potential energy in the NbO_x species). For the fundamentals, the presence of only one band will indicate a mono-oxo species because such a two-atom system has only one stretching mode (ν_s). Conversely, the fundamental stretching region of a di-oxo species will have two bands due to the symmetric (ν_s) and asymmetric (ν_{as}) stretching modes of the triatomic system. These frequencies should be separated by about 10–30 cm^{-1}, according to several authors.[47–49] Furthermore, for the di-oxo species the symmetric mode will be more intense in Raman, while the asymmetric mode will dominate in IR. In the overtone region, only one overtone band will appear for a mono-oxo diatom ($2\nu_s$). However, three bands should appear for a di-oxo triatomic system—one overtone each for the symmetric ($2\nu_s$) and asymmetric ($2\nu_{as}$) modes, as well as a combination band ($\nu_s + \nu_{as}$).

Based on the coincident frequency of the IR and Raman fundamental that occurs at ∼980 cm^{-1} in Nb_2O_5/Al_2O_3, Nb_2O_5/ZrO_2, and Nb_2O_5/TiO_2, it appears that this band arises from a mono-oxo species. A di-oxo species, with the most intense Raman band being the symmetric Nb=O stretch at ∼980 cm^{-1}, would exhibit the most intense IR fundamental for the asymmetric stretch at a frequency different than ∼980 cm^{-1}. For example, if the relatively weaker Raman band at ∼935 cm^{-1} in Nb_2O_5/ZrO_2 was taken to be the asymmetric stretch of the di-oxo species, then this band would be the most intense IR fundamental. Instead, the most intense Raman and IR fundamentals occur at exactly the same frequency of ∼980 cm^{-1}, which excludes the presence of a di-oxo species. Additionally, the frequency shifts observed with loading are similar in Raman as in IR: the fundamental Nb=O band shifts from ∼980 to ∼988 cm^{-1} in Nb_2O_5/Al_2O_3 and from ∼965 cm^{-1} to ∼980 cm^{-1} in Nb_2O_5/ZrO_2 and remains constant with loading at ∼978 cm^{-1} in Nb_2O_5/TiO_2. Thus, the coincidence of IR and Raman

IR Spectra of Niobium Oxide Catalysts

J. Phys. Chem. B, Vol. 103, No. 29, 1999 **6021**

frequencies, frequency shifts, and relative intensities for the Nb=O fundamental stretching band at 980 cm^{-1} strongly suggests that this band represents a mono-oxo species.

The overtones of Nb$_2$O$_5$/TiO$_2$ and Nb$_2$O$_5$/ZrO$_2$ are also consistent with a mono-oxo structure, since only a single overtone is observed at very nearly twice the frequency of the ~980 cm^{-1} fundamental (~1960 cm^{-1}). These overtones shift with loading in accordance with the fundamental shifts observed in Raman and IR (see Table 2). Recall that for Nb$_2$O$_5$/TiO$_2$, the second, less intense overtone band at 1986 cm^{-1} was assigned to Nb$_2$O$_5$·nH$_2$O (see Results section and Figure 1). For Nb$_2$O$_5$/Al$_2$O$_3$, the strongest overtone band also occurs at twice the frequency of the 988 cm^{-1} Raman fundamental (1966 cm^{-1}), and this overtone similarly shifts with loading in the same way as the Raman fundamental (see Table 2). Again, the fact that the most intense IR overtone corresponds to twice the frequency of (and shifts with niobia loading in the same way as) the coincident Raman and IR fundamental is strong evidence for a mono-oxo assignment of the 980 cm^{-1} band. Jehng and Wachs,[15,39] Pittman and Bell,[17] and Ko et al.[8,40] have made the same mono-oxo assignment for the 980 cm^{-1} fundamental band based on vibrational spectra.

Mono-oxo structures have also been found on other supported metal oxide systems. For example, in several supported metal oxide catalysts[37,49] the exchange of some fraction of the terminal M=O (M = W, Mo, V, and Cr) bonds with oxygen-18 indicated a mono-oxo structure because only two vibrational bands were detected for M=^{16}O and M=^{18}O. A di-oxo structure would have exhibited a third band due to the ^{16}O=M=^{18}O structure. Unfortunately, preliminary oxygen-18 exchange experiments[50] on supported niobia catalysts have not succeeded due to the difficulty involved in reducing the supported niobia species prior to reoxidation in ^{18}O$_2$. Nevertheless, the present use of comparative IR/Raman studies for the discrimination of mono-oxo versus di-oxo structures on supported niobia catalysts is equally effective, and such comparative methods have also been used to show mono-oxo structures on supported WO$_3$, MoO$_3$, V$_2$O$_5$, and CrO$_3$ catalysts.[18,35,37,47,49,51,52] Last, it is difficult to account for the di-oxo structures presented by some authors from EXAFS data[10,20,22-23] because the preparation method of supported niobia catalysts has been shown not to affect the molecular structure.[11,13] However, the discrepancy may be due to ambiguities involved in the complex curve-fitting analysis employed in the EXAFS studies (see, for example, the discussion of 19 wt % Nb$_2$O$_5$/Al$_2$O$_3$ EXAFS data by Tanaka et al.[23]).

The fundamental region of Nb$_2$O$_5$/ZrO$_2$ and the overtone region of Nb$_2$O$_5$/Al$_2$O$_3$ provide additional information about the lower frequency fundamentals at ~935 and ~880 cm^{-1}. This is because the ZrO$_2$ support maintains an exceptionally large fundamental transmission window to about ~800 cm^{-1}. Also, the lower frequency overtone and combination bands on alumina are observed because of the much higher concentration of niobia on alumina (15 wt %) compared to the niobia concentration on TiO$_2$ (7 wt %) and ZrO$_2$ (5 wt %). From the Raman spectra,[15] all three fundamental bands were previously assigned to mono-oxo, Nb=O stretching vibrations within different types of surface species: isolated NbO$_x$ surface species with Nb=O bonds that are short (985 cm^{-1}) and long (883 cm^{-1}), and polymerized NbO$_x$ species with intermediate Nb=O bond lengths (935 cm^{-1}). The IR results of the current investigation support this assignment for the 980 cm^{-1} fundamental, as was discussed above. However, the IR band at 1914 cm^{-1} in the overtone region of Nb$_2$O$_5$/Al$_2$O$_3$ appears to be the combination of the 935 + 980 cm^{-1} fundamentals. The presence of such a combination band argues against assignment of these fundamentals to separate Nb=O species because fundamentals must belong to the same symmetry group in order to produce a combination mode.[34]

These lower frequency fundamentals (935 and 880 cm^{-1}) are more likely due to stretching modes of Nb—O—Nb bonds in polymerized NbO$_x$ species, the presence of which has been indicated by EXAFS studies[10,22-23,26] and, at high loadings, by a Raman band[15,17] at ~650 cm^{-1}. Several other authors have also assigned IR and Raman bands in the 700-900 cm^{-1} region to Nb—O—Nb modes in bridged niobia compounds,[39,53] Nb$_2$O$_5$/TiO$_2$ catalysts,[17] and Nb$_2$O$_5$/SiO$_2$ catalysts.[8] Also, in supported chromia systems, Vuurman et al.[35] assigned the rather intense Raman mode at 880 cm^{-1} to the symmetric stretch, ν_s, of [—O—Cr—O—]$_n$ polymerized bonds, while the band at ~600 cm^{-1} was assigned to the symmetric stretch of Cr—O—Cr vibrations. Other authors[37,51-52,54-57] have assigned similar Raman bands at ~880 cm^{-1} to M—O—M linkages in WO$_3$/Al$_2$O$_3$, MoO$_3$/Al$_2$O$_3$, V$_2$O$_5$/Al$_2$O$_3$, and WO$_3$/TiO$_2$. Furthermore, it was shown that the 880 cm^{-1} Raman band in V$_2$O$_5$/Al$_2$O$_3$, which is present at low loading, shifts to 935 cm^{-1} at high loading.[18] Similar shifts of the 880 cm^{-1} band to higher frequencies were also observed[18,57] for WO$_3$/Al$_2$O$_3$ and MoO$_3$/Al$_2$O$_3$. The Raman spectra of Nb$_2$O$_5$ on alumina, zirconia, and titania also show an 880 cm^{-1} band at low loading and a 935 cm^{-1} band at high loading,[15] as does the IR spectrum of Nb$_2$O$_5$/ZrO$_2$ (Figure 3A,C). Thus, it seems that the fundamental niobia bands at 880 and 935 cm^{-1} are, in fact, due to the same ν_s([—O—Nb—O—]$_n$) stretching mode in polymerized Nb—O—Nb bonds, which shifts to higher frequency with surface niobia coverage.

Some additional evidence further supports assignment of the 935 cm^{-1} band to [—O—Nb—O—]$_n$ bridging bonds, despite the fact that previous authors have assigned the 935 cm^{-1} band to mono-oxo Nb=O terminal bonds within polymeric niobia chains based on comparisons with reference niobium compounds.[15,17-18] First, the presence of the previously mentioned combination band at 1914 cm^{-1} (980 + 935 cm^{-1}), which was observed on 15 wt % Nb$_2$O$_5$/Al$_2$O$_3$, suggests that the structural moieties giving rise to the 980 and 935 cm^{-1} bands are connected in close enough proximity to each other that they belong to the same (unknown) symmetry group. The 980 cm^{-1} band was also shown to be mono-oxo, and it is unlikely that two different mono-oxo Nb=O units, vibrating separately at 980 and 935 cm^{-1} and joined by a bridging oxygen, would form a symmetry group with sufficient vibrational coupling to produce a combination band. In other words, localization of the potential energy on the Nb=O groups in such a structure would, from a symmetry perspective, effectively isolate the niobyl groups. However, an [—O—Nb—O—]$_n$ stretching mode at 935 cm^{-1}, in which the Nb atoms also simultaneously belong to Nb=O units vibrating at 980 cm^{-1}, could reasonably be expected to produce a combination mode at 1914 cm^{-1}. Second, the Raman and IR bands at 935 cm^{-1} are significantly broader than the Nb=O bands at 980 cm^{-1}, and broad bands are typical of the wide distribution of bond and chain lengths found in metal—oxygen—metal polymerized bonds.[17,35,53] Finally, structural distortions in monolayer-type surface species generally cause an upward shift (shortening of bond lengths) in metal—oxygen vibrations as loading is increased.[18,37,51,55] This behavior is seen, for example, in the shift of the mono-oxo Nb=O stretching mode from somewhat lower frequency to 988 cm^{-1} in Nb$_2$O$_5$/Al$_2$O$_3$ and Nb$_2$O$_5$/ZrO$_2$ (see Table 2). Shifts to higher wavenumber with increased loading might also be expected for the polym-
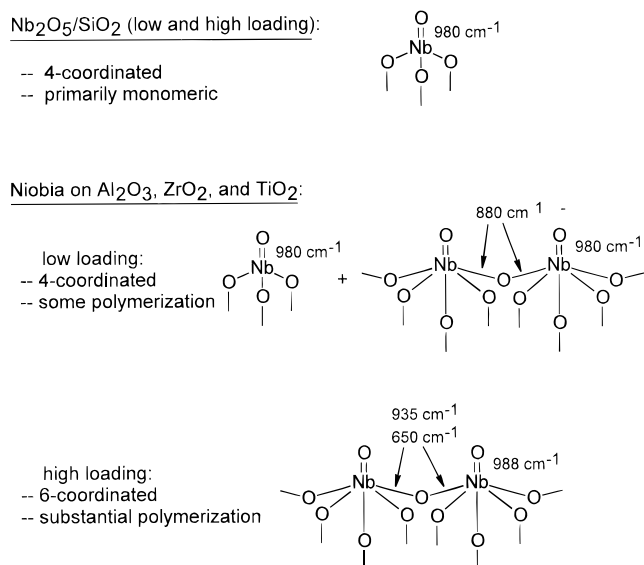
Figure 7. Schematic drawing of the molecular structures present on supported niobia catalysts under dehydrated conditions. Assignments of the Nb—O—Nb modes, by analogy to assignments in supported chromia systems,[35] include assignment of the vibrational band at ~880–935 cm^{-1} to $\nu_s([-O-Nb-O-]_n)$, while the band at ~650 cm^{-1} is assigned to $\nu_s(Nb-O-Nb)$.

erized $[-O-Nb-O-]_n$ mode, i.e., shifting from 880 cm^{-1} at low niobia loading to 935 cm^{-1} at monolayer coverage.

These assignments are illustrated schematically with the molecular structures of the supported niobia species in Figure 7. Also indicated in the figure is the variation in coordination and degree of polymerization with niobia loading. The coordination of surface niobia species was originally argued to be entirely octahedral (NbO$_6$) based on the frequency of the Nb= O Raman band relative to reference compounds and on some theoretical observations concluding that the effective Nb^{5+} valence state and size were inappropriate for tetrahedral NbO$_4$ units.[15,17] However, other authors[8,17] note that Nb^{5+} size constraints in NbO$_4$ tetrahedra may not be critical for dispersed niobia surface species that lack close-packing of oxygen around the Nb^{5+} atom. Horsley et al.[56] have also pointed out that the determination of coordination solely from metal—oxygen (M= O) Raman stretching frequencies is not completely conclusive in the region 910–980 cm^{-1}.

In fact, the present results show that the Nb=O stretching frequency in supported niobia catalysts is generally not very sensitive to the niobium coordination or to the specific oxide support (see Table 2). Only slight shifts in the fundamental Nb= O band are observed at 980–988 cm^{-1} and at 983–985 cm^{-1} for Nb$_2$O$_5$/Al$_2$O$_3$ and Nb$_2$O$_5$/TiO$_2$, respectively, while the band position remains constant at 988 cm^{-1} for Nb$_2$O$_5$/SiO$_2$. This insensitivity to coordination change and support, which has also been observed as a general phenomenon on other supported metal oxide systems,[37] is most likely due to the localization and concentration of NbO$_x$ vibrational potential energy in the Nb=O double bond. Such vibrationally isolated Nb=O diatomic units will not be strongly influenced by less energetic Nb—O vibrations in the larger NbO$_4$ or NbO$_6$ units, and Hardcastle and Wachs[19] successfully used this diatomic approximation to correlate bond lengths and bond strengths with Nb=O Raman stretching frequencies in bulk and supported niobia systems. In agreement with the present results, these authors also found a rather ambiguous relationship between Nb=O Raman stretching frequencies and niobium coordination. For Nb$_2$O$_5$/ZrO$_2$, the relatively low Nb=O fundamental vibration present at low

loading at 956 cm^{-1} (R)/965 cm^{-1} (IR) suggests that the Nb= O bond on this catalyst is somewhat less energetic and more susceptible to influence by coordination changes or to the zirconia support. However, at monolayer coverage this band shifts upward to the same 988 cm^{-1} position seen on the other catalysts, again indicating that the Nb=O bond is vibrationally isolated because it is independent of support. The overtone Nb= O band positions are also consistent with vibrationally isolated Nb=O bonds, where the slightly larger shift in the Nb$_2$O$_5$/Al$_2$O$_3$ overtones relative to the shift in the corresponding fundamentals is likely due to anharmonicity effects.

At any rate, sufficient XANES data have been presented[23,24] to indicate the presence of 4-fold coordination for niobia species in Nb$_2$O$_5$/SiO$_2$ at all loadings and in Nb$_2$O$_5$/Al$_2$O$_3$ for low loadings. Six-fold coordination is found by XANES[23] for high loadings of Nb$_2$O$_5$/Al$_2$O$_3$, in agreement with the previous conclusions drawn from Raman data. As mentioned previously for Nb$_2$O$_5$/Al$_2$O$_3$, an increase in the degree of polymerization with increased niobia loading is indicated by the growth of a vibrational band at ~650 cm^{-1}, by a shift in the polymerized band at 880 cm^{-1} (low loading) to 935 cm^{-1} (high loading), and by EXAFS studies.[23] However, some Nb—O—Nb structures are also indicated at low loading by the 880 cm^{-1} IR and Raman bands, and again by EXAFS.[23] The presence of such polymerized Nb—O—Nb bonds is nearly always associated with 6-fold coordination,[39] so their presence on Nb$_2$O$_5$/TiO$_2$ and Nb$_2$O$_5$/ ZrO$_2$ suggests that the coordination behavior of these catalysts should be analogous to that of Nb$_2$O$_5$/Al$_2$O$_3$. An exception is silica-supported niobia, which is considerably more monomeric in nature based on the absence of a niobia Raman band[15] at 880–935 cm^{-1} and on EXAFS studies[24] that show very little aggregation of niobia surface species below monolayer coverage (aggregated Nb$_2$O$_5$ microcrystallites form above monolayer coverage[15,24]). A similar conclusion of 4-fold surface monomers has also been recently presented for silica-supported vanadia[38] and chromia[35] using a variety of characterization techniques.

2. Interactions between Support Hydroxyls and NbO$_x$ Surface Species. A second objective of this study is the determination of the nature of the interaction between the support surface hydroxyls and the deposited surface niobia overlayer. Numerous authors[7,17,33,35–38] have shown that deposition of acidic transition metal oxides such as the oxides of Cr, V, Mo, Nb, Re, and W onto oxide supports generally occurs via titration of the support hydroxyls. This acid—base reaction preferentially titrates the more basic support hydroxyls that generally vibrate at higher frequencies. For example, deposition of chromia[35] and vanadia[38] on silica resulted in the diminishing of isolated Si—OH groups, while the geminal hydroxyls were not affected. This is in agreement with the present results for niobia on silica and indicates that the isolated silanols are more reactive with niobia than are the geminal hydroxyls (Figure 5A). In Nb$_2$O$_5$/Al$_2$O$_3$, the most basic hydroxyls of the highest stretching frequency are also the most reactive with niobia (Figure 5B), but significant amounts of less basic hydroxyls remain unreacted even at the highest niobia loading (corresponding to ~80% of monolayer surface coverage). The Nb$_2$O$_5$/ ZrO$_2$ system generally follows this same trend (Figure 5C), since the highest frequency hydroxyl band at 3769 cm^{-1} nearly vanishes at the highest loading of niobia. However, a new band appears at 3710–3730 cm^{-1} with increased niobia loading that is very similar in frequency to the Nb—OH band present on bulk Nb$_2$O$_5$·nH$_2$O at 3702 cm^{-1} (Figure 6). For Nb$_2$O$_5$/TiO$_2$, the shift with niobia loading of the 3720 cm^{-1} isolated Ti—OH band to 3710 cm^{-1} (Figure 5D) also suggests the creation of a

IR Spectra of Niobium Oxide Catalysts

J. Phys. Chem. B, Vol. 103, No. 29, 1999 **6023**

new surface Nb—OH band at 3710 cm^{-1} and is consistent with the expected preferential titration of the higher frequency Ti—OH band at 3720 cm^{-1} by the deposited niobia. In all cases, a significant population of support hydroxyls remains even at monolayer coverages, indicating that not all support OH groups are accessible or reactive with deposited niobia.

The growth of a band at 3710—3730 cm^{-1} in Nb$_2$O$_5$/ZrO$_2$ and Nb$_2$O$_5$/TiO$_2$ with increased niobia loading is especially interesting because it indicates that new surface hydroxyls (absent in the support itself) are formed upon reaction of the support with niobia. However, the exact interpretation of this band is not presently known—it may be due to either Nb—OH or Nb—OH—Zr (Nb—OH—Ti) species. This new band does have a slightly higher frequency than the Nb—OH band at 3702 cm^{-1} in bulk Nb$_2$O$_5$·nH$_2$O, which means that the bond length of this hydroxyl is somewhat shorter than that of Nb—OH in niobic acid. However, earlier studies[6] with pyridine adsorption have shown that neither Nb$_2$O$_5$/ZrO$_2$ nor Nb$_2$O$_5$/TiO$_2$ contain Brønsted acid sites, so it is likely that the 3710—3730 cm^{-1} hydroxyls are not strongly acidic. It would also be quite interesting to ascertain whether the new hydroxyl group present on Nb$_2$O$_5$/ZrO$_2$ and Nb$_2$O$_5$/TiO$_2$ is unique for these systems or occurs for niobia deposited on other supports, as well. However, the intensities of the Si—OH and Al—OH hydroxyls, even at monolayer coverages of niobia, are substantially higher than that of any new band in the region 3710—3730 cm^{-1} (based on the intensities of this band in Nb$_2$O$_5$/ZrO$_2$ and Nb$_2$O$_5$/TiO$_2$). Nevertheless, niobia deposition on Al$_2$O$_3$ and SiO$_2$ at high coverages resulted in either increased absorption in this region (SiO$_2$) or in the relative domination of an existing support band in this region that could be due to coincidental overlap of the support hydroxyl and new hydroxyl frequencies (Al$_2$O$_3$). Therefore, such a band from a new hydroxyl species may be obscured in these supported niobia systems.

Conclusions

Analysis of the infrared and Raman spectra of bulk Nb$_2$O$_5$·nH$_2$O and supported niobium oxide catalysts (Nb$_2$O$_5$/SiO$_2$, Nb$_2$O$_5$/Al$_2$O$_3$, Nb$_2$O$_5$/ZrO$_2$, and Nb$_2$O$_5$/TiO$_2$) have yielded valuable information about the molecular structures of the dehydrated niobia surface species. The coincidence of IR and Raman fundamental frequencies in Nb$_2$O$_5$/Al$_2$O$_3$, Nb$_2$O$_5$/ZrO$_2$, and Nb$_2$O$_5$/TiO$_2$ provides the strongest evidence that the NbO$_x$ surface species (Nb=O fundamental at 980 cm^{-1}) is present as a mono-oxo moiety. A di-oxo species would not have coincident IR and Raman fundamental frequencies. This conclusion is further supported by the presence of only a single overtone at ∼1960 cm^{-1} in Nb$_2$O$_5$/ZrO$_2$ and Nb$_2$O$_5$/TiO$_2$, and the presence of the most intense overtone at 1966 cm^{-1} in Nb$_2$O$_5$/Al$_2$O$_3$. Therefore, the 980 cm^{-1} fundamental vibrational mode is best assigned to a mono-oxo Nb=O species.

In the case of Nb$_2$O$_5$/ZrO$_2$, the lower frequency fundamentals at 880 cm^{-1} (low loading) and 935 cm^{-1} (high loading) are also seen to be coincident with the Raman fundamentals, and these lower frequency fundamentals were similarly seen in Raman spectra for Nb$_2$O$_5$ on alumina and titania. Additionally, the overtone region of Nb$_2$O$_5$/Al$_2$O$_3$ exhibited weak bands at ∼1914 and 1870 cm^{-1}. The band at 1870 cm^{-1} is assigned to the overtone of the 935 cm^{-1} fundamental vibration (observed in Raman for Nb$_2$O$_5$/Al$_2$O$_3$), and the band at 1914 cm^{-1} is assigned to the combination of the 935 + 980 cm^{-1} fundamentals. More importantly, the presence of such a combination mode indicates that the 980 and 935 cm^{-1} fundamentals belong to the same symmetry group and not to separate Nb=O units on

different NbO$_x$ species. Instead, similar behavior observed on other supported metal oxide systems (oxides of V, Cr, Mo, and W on various oxide supports[35,37,51−52,54−57]) indicates that the fundamental niobia bands at 880 and 935 cm^{-1} should be assigned to an Nb—O—Nb stretching mode, $\nu_s([-O-Nb-O-]_n)$, that shifts from 880 to 935 cm^{-1} with increased loading. Finally, observation of the hydroxyl region indicates that the higher frequency surface hydroxyls on the SiO$_2$, Al$_2$O$_3$, ZrO$_2$, and TiO$_2$ supports are generally titrated preferentially as niobia loading is increased. Also, in Nb$_2$O$_5$/ZrO$_2$ and Nb$_2$O$_5$/TiO$_2$ a new (nonacidic or weakly acidic) Nb—OH or Nb—OH—Zr (Nb—OH—Ti) surface hydroxyl group is created at 3710—3730 cm^{-1}, which is very similar in frequency to the Nb—OH band observed in bulk Nb$_2$O$_5$·nH$_2$O at 3702 cm^{-1}.

References and Notes

(1) Jehng, J.-M.; Wachs, I. E. *High Temp. Mater. Proc.* **1993**, *11*, 159.

(2) See papers in special niobium issues of *Catal. Today*: (a) **1990**, *8*. (b) **1993**, *16*. (c) **1996**, *28*.

(3) Tanaka, T.; Takenaka, S.; Funabiki, T.; Yoshida, S. *Chem. Lett.* **1994**, 809.

(4) Jehng, J.-M.; Turek, A. M.; Wachs, I. E. *Appl. Catal. A* **1992**, *83*, 179.

(5) Okazaki, S.; Okuyama, T. *Bull. Chem. Soc. Jpn.* **1983**, *56*, 2159.

(6) Datka, J.; Turek A. M.; Jehng, J.-M.; Wachs, I. E. *J. Catal.* **1992**, *135*, 186.

(7) Turek, A. M.; Wachs, I. E.; DeCanio, E. *J. Phys. Chem.* **1992**, *96*, 5000.

(8) Burke, P. A.; Ko, E. I. *J. Catal.* **1991**, *129*, 38.

(9) Maurer, S. M.; Ng, D.; Ko, E. I. *Catal. Today* **1993**, *16*, 319.

(10) Shirai, M.; Ichikuni, N.; Asakura, K.; Iwasawa, Y. *Catal. Today* **1990**, *8*, 57.

(11) Wachs, I. E.; Jehng, J.-M.; Deo, G.; Hu, H.; Arora, N. *Catal. Today* **1996**, *28*, 199.

(12) Jehng, J.-M.; Wachs, I. E. *Catal. Today* **1990**, *8*, 37.

(13) Jehng, J.-M.; Wachs, I. E. *Catal. Today* **1993**, *16*, 417.

(14) Bernholc, J.; Horsley, J. A.; Murrell, L. L.; Sherman, L. G.; Soled, S. *J. Phys. Chem.* **1987**, *91*, 1526.

(15) Jehng, J.-M.; Wachs, I. E. *J. Phys. Chem.* **1991**, *95*, 7373.

(16) Jehng, J.-M.; Wachs, I. E. *J. Mol. Catal.* **1991**, *67*, 369.

(17) Pittman, R. M.; Bell, A. T. *J. Phys. Chem.* **1993**, *97*, 12178.

(18) (a) Vuurman, M. A.; Wachs, I. E. *J. Phys. Chem.* **1992**, *96*, 5008. (b) Vuurman, M. A. Ph.D. Dissertation, University of Amsterdam, The Netherlands, 1992.

(19) Hardcastle, F. D.; Wachs, I. E. *Solid State Ionics* **1991**, *45*, 201.

(20) Nishimura, M.; Asakura, K.; Iwasawa, Y. *J. Chem. Soc., Chem. Commun.* **1986**, 1660.

(21) Yoshida, S.; Tanaka, T.; Hanada, T.; Hiraiwa, T.; Kanai, H.; Funabiki, T. *Catal. Lett.* **1992**, *12*, 277.

(22) Ichikuni, N.; Shirai, M.; Iwasawa, Y. *Catal. Today* **1996**, *28*, 49.

(23) Tanaka, T.; Yoshida, T.; Yoshida, H.; Aritani, H.; Funabiki, T.; Yoshida, S.; Jehng, J.-M.; Wachs, I. E. *Catal. Today* **1996**, *28*, 71.

(24) Yoshida, H.; Tanaka, T.; Yoshida, T.; Funabiki, T.; Yoshida, S. *Catal. Today* **1996**, *28*, 79.

(25) Yoshida, S.; Nishimura, Y.; Tanaka, T.; Kanai, H.; Funabiki, T. *Catal. Today* **1990**, *8*, 67.

(26) Ichikuni, N.; Iwasawa, Y. *Catal. Today* **1993**, *16*, 427.

(27) Hasegawa, S.; Aritani, H.; Kudo, M. *Catal. Today* **1993**, *16*, 371.

(28) Kobayashi, H.; Yamaguchi, M.; Tanaka, T.; Nishimura, Y.; Kawakami, H.; Yoshida, S. *J. Phys. Chem.* **1988**, *92*, 2516.

(29) Weissman, J. G.; Ko, E. I.; Wynblatt, P.; Howe, J. M. *Chem. Mater.* **1989**, *1*, 187.

(30) Weissman, J. G.; Ko, E. I.; Wynblatt, P. *J. Catal.* **1987**, *108*, 383.

(31) Ko, E. I.; Bafrali, R.; Nuhfer, N. T.; Wagner, N. J. *J. Catal.* **1985**, *95*, 260.

(32) Tanaka, T.; Nojima, H.; Yoshida, H.; Nakagawa, H.; Funabiki, T.; Yoshida, S. *Catal. Today* **1993**, *16*, 297.

(33) Nishimura, M.; Asakura, K.; Iwasawa, Y. *Chem. Lett.* **1986**, 1457.

(34) Nakamoto, K. *Infrared and Raman Spectra of Inorganic and Coordination Compounds*, 4th ed.; John Wiley & Sons: New York, 1986.

(35) Vuurman, M. A.; Wachs, I. E.; Stufkens, D. J.; Oskam, A. *J. Mol. Catal.* **1993**, *80*, 209.

(36) Wachs, I. E. *Colloids Surf. A* **1995**, *105*, 143.

(37) Wachs, I. E. *Catal. Today* **1996**, *27*, 437.

(38) Gao, X.; Bare, S. R.; Weckhuysen, B. M.; Wachs, I. E. *J. Phys. Chem. B* **1998**, *102*, 10842.

(39) Jehng, J.-M.; Wachs, I. E. *Chem. Mater.* **1991**, *3*, 100.

(40) Maurer, S. M.; Ko, E. I. *J. Catal.* **1992**, *135*, 125.

(41) Hair, M. L.; Hertl, W. *J. Phys. Chem.* **1969**, *73*, 2372.

(42) (a) Knözinger, H.; Ratnasamy, P. *Catal. Rev. Sci. Eng.* **1978**, *17*, 31. (b) Boehm, H. P.; Knözinger, H. in *Catalysis: Science and Technology*; Anderson, J. R., Boudart, M., Eds.; Springer-Verlag: New York, 1983; Vol. 4.

(43) Tsyganenko, A. A.; Filimonov, V. N. *J. Mol. Struct.* **1973**, *19*, 579.

(44) Primet, M.; Pichat, P.; Mathieu, M.-V. *J. Phys. Chem.* **1971**, *75*, 1216.

(45) (a) Odenbrand, C. U. I.; Andersson, S. L. T.; Andersson, L. A. H.; Brandin, J. G. M.; Busca, G. *J. Catal.* **1990**, *125*, 541. (b) Busca, G.; Saussey, H.; Saur, O.; Lavalley, J. C.; Lorenzelli, V. *Appl. Catal.* **1985**, *14*, 245.

(46) Deo, G.; Turek, A. M.; Wachs, I. E.; Machej, T.; Haber, J.; Das, N.; Eckert, H.; Hirt, A. M. *Appl. Catal. A* **1992**, *91*, 27.

(47) (a) Cristiani, C.; Forzatti, P.; Busca, G. *J. Catal.* **1989**, *116*, 586. (b) Wachs, I. E. *J. Catal.* **1990**, *124*, 570. (c) Ramis, G.; Cristiani, C.; Forzatti, P.; Busca, G. *J. Catal.* **1990**, *124*, 574.

(48) (a) Ahlborn, E.; Diemann, E.; Müller, A. *Z. Anorg. Allg. Chem.* **1972**, *394*, 1. (b) Sathyanarayana, D. N.; Patel, C. C. *Bull. Chem. Soc. Jpn.* **1964**, *37*, 1736. (c) Soptrajanov, B.; Nikolovskii, A.; Petrov, I. *Spectrochim. Acta, Part A* **1968**, *24A*, 1617.

(49) Weckhuysen, B. M.; Wachs, I. E. *J. Phys. Chem. B* **1997**, *101*, 2793.

(50) Burcham, L. J.; Wachs, I. E. unpublished TPR and Raman results.

(51) Kim, D. S.; Ostromecki, M.; Wachs, I. E. *J. Mol. Catal. A* **1996**, *106*, 93.

(52) Ramis, G.; Busca, G.; Cristiani, C.; Lietti, L.; Forzatti, P.; Bregani, F. *Langmuir* **1992**, *8*, 1744.

(53) Katovic, V.; Djordjevic, C. *Inorg. Chem.* **1970**, *9*, 1720.

(54) (a) Stencel, J. M.; Makovsky, L. E.; Diehl, J. R.; Sarkus, T. A. *J. Catal.* **1985**, *95*, 414. (b) Vuurman, M. A.; Stufkens, D. J.; Oskam, A.; Deo, G.; Wachs, I. E. *J. Chem. Soc., Faraday Trans.* **1996**, *92*, 3259.

(55) Jehng, J.-M.; Deo, G.; Weckhuysen, B. M.; Wachs, I. E. *J. Mol. Catal. A* **1996**, *110*, 41.

(56) Horsley, J. A.; Wachs, I. E.; Brown, J. M.; Via, G. H.; Hardcastle, F. D. *J. Phys. Chem.* **1987**, *91*, 4014.

(57) Ostromecki, M. M.; Burcham, L. J.; Wachs, I. E. *J. Mol. Catal. A* **1998**, *132*, 59.